Polymer Journal, Vol. 25, No. 12, pp 1235—1245 (1993)

Mean End-to-End Distance of a Polymer Confined between Two Interacting Plates

Kohzoh SHIOKAWA

Department of Applied Science, Faculty of Engineering, Kyushu University, Hakozaki, Higashi-ku, Fukuoka 812, Japan

(Received February 4, 1993)

ABSTRACT: The mean end-to-end distance of a polymer confined between two plates, and interaction with the plates, were studied in the presence of excluded volume interaction. The polymer surface interaction is included exactly in the unperturbed distribution function of the confined polymer as the boundary condition. The excluded volume interaction is introduced perturbatively using the homotopy parameter expansion method. The component of the mean square end to end distance parallel to the plates is calculated as the function of DW and $D/\langle R_z^2\rangle_\infty^{1/2}$, where D is the interplate distance, W is the the polymer-plate interaction parameter and $\langle R_z^2\rangle_\infty$ is the component of the mean square end to end distance perpendicular to the plates in an unconfined state. It was found that the attractive interaction between the polymer and the plates has a larger effect on chain dimensions than the repellent interaction between them. The parallel components of the mean end-to-end distance of the chain where one end is fixed at an assigned position is also calculated.

KEY WORDS End-to-End Distance / Confined Polymer / Slit / Slab / Excluded Volume / Renormalization Group Theory / Homotopy Parameter Expansion / Adsorption /

The conformational properties of a polymer interacting with a surface are relevant to many practical problems such as adhesion, stabilization of colloid particles and reinforcement. Many theoretical studies have been carried out.[1] A polymer confined between two plates, and interacting with the plates, has also been studied. However, most of these reports deal with systems in which one end, or else some parts of the polymers are anchored on the plate. The effects of the polymer surface interaction on the conformational properties were studied by DiMarzio and Rubin[2] using lattice models and by Chan, Davis and Richmond[3] using a continuum model. However, the full dependencies of the polymer surface interaction from an unconfined state to a confined state have not yet been studied.

The excluded volume interaction has a strong influence on chain dimensions not only in an unconfined state but also in a confined state.The excluded volume interaction further complicates the calculation of chain dimensions. There are a few studies dealing with the effects of both the excluded volume interaction and polymer surface interaction on chain conformations. Daoud and de Gennes[4] and Turban[5] discussed the dimensions of a confined chain using scaling arguments. However, they did not study the effect of polymer plate interaction. Wang, Nemirovsky and Freed[6] investigated chain dimensions using the ε expansion method for cases of a polymer confined between two perfectly repellent plates and between two reflecting plates. The present author derived the full dependence of the chain dimensions of a confined chain on the interplate distance, using the homotopy parameter ex-

pansion method[7] and mean field theory[8] for cases in which a polymer is confined between two perfectly repellent plates.

In this paper, we studied the full dependence of the mean end-to-end distance of a confined polymer on the interplate distance, and on the polymer surface interaction in the presence of the excluded volume. The polymer surface interaction is included exactly within the distribution functions of the unperturbed polymer confined between two plates. The excluded volume interaction is then introduced perturbatively using the homotopy parameter expansion method proposed by Oono.[9]

MODEL

A model chain consists of N_0 freely jointed bonds of a unit length. The interplate distance, D, is much larger than unity, so the continuous polymer chain model can be utilized. The z axis is taken perpendicular to the plates and the x and y axes are taken parallel to the plates. The polymer chain is confined between $z=-D/2$ and $D/2$.

The probability distribution function of an unperturbed chain which starts at $\boldsymbol{R}'$ and ends at $\boldsymbol{R}$, satisfies the following differential equation.

$$\left(\frac{\partial}{\partial N_0}-\frac{1}{6}\nabla^2\right)G_0(\boldsymbol{R}, \boldsymbol{R}'; N_0)=\delta(\boldsymbol{R}-\boldsymbol{R}')\delta(N_0) \tag{1}$$

On the atomic scale, interaction between the polymer and the plates depends on the local conformations of the polymer at the plates, and on the fine structures of the plate surfaces. However it is too difficult to introduce their contributions in the distribution function. We disregard these fine structures, and assume that the interaction has effects only on bonds in the vicinity of the plate surfaces. Thus the interaction is introduced as a boundary condition for eq 1 according to deGennes[10]

$$(\partial G_0/\partial z)/G_0=\mp W \qquad \text{at} \quad z=\pm D/2 \tag{2}$$

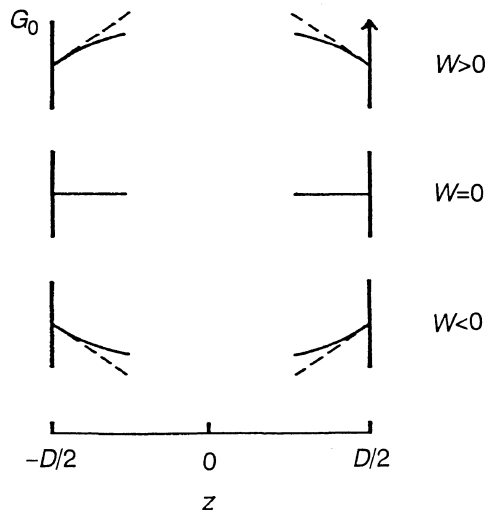

Figure 1. Schematic diagram of the polymer plate interaction parameter. Top, repellent surface; middle, reflecting surface; bottom, attractive surface.

where W is the polymer plate interaction parameter per unit length. The schematic diagram of eq 2 is given in Figure 1. For positive values of W, segment concentration in the bulk state is richer than that on the surface. A positive value of W thus means that the polymer surface interaction is repellent. In contrast, a negative value of W corresponds to attractive interaction.

From eq 1 and 2, G_0 is translationally invariant for x and y directions. Then G_0 can be decomposed as

$$G_0(\boldsymbol{R}, \boldsymbol{R}'; N_0) = G_{0x}(R_x; N_0)G_{0y}(R_y; N_0)G_{0z}(z, z'; N_0) \tag{3}$$

where R_x and R_y are the components of the end-to-end vector parallel to the plates. For an unperturbed chain, G_{0x} and G_{0y} are Gaussian functions.

Solving eq 1 under the boundary conditions of eq 2, we get the component of distribution function perpendicular to the plates, G_{0z} as follows:

$$G_{0z}(z, z'; N_0)$$
$$= \frac{2}{D}\left\{\sum_k A_k \cos\left(\frac{a_k z}{D}\right)\cos\left(\frac{a_k z'}{D}\right)\exp(-a_k^2 d_0)\right.$$
$$+\sum_k B_k \sin\left(\frac{b_k z}{D}\right)\sin\left(\frac{b_k z'}{D}\right)\exp(-b_k^2 d_0)$$
$$+A\cosh\left(\frac{az}{D}\right)\cosh\left(\frac{az'}{D}\right)\exp(a^2 d_0)$$
$$\left.+B\sinh\left(\frac{bz}{D}\right)\sinh\left(\frac{bz'}{D}\right)\exp(b^2 d_0)\right\} \quad (4)$$

where $d_0 = N_0/6D^2$. The coefficients a_k, b_k, a, and b are determined by the following transcendental equations, where A_k, B_k, A, and B are normalization constants:

$$\tan(a_k/2) = DW/a_k; \quad A_k = 1/(1+\sin(a_k)/a_k) \quad (5a)$$

$$\cot(b_k/2) = -DW/b_k; B_k = 1/(1-\sin(b_k)/b_k) \quad (5b)$$

$$\tanh(a/2) = -DW/a; A = 1/(\sinh(a)/a+1) \quad (5c)$$

$$\coth(b/2) = -DW/b; B = 1/(\sinh(b)/b-1) \quad (5d)$$

The nature of the roots, a_k and b_k is demonstrated in Figure 2. This illustrates the curves corresponding to the right- and left-hand sides of eq 5a and 5b, respectively. For given DW, the values of abscissas of intersecting points correspond to a_k or b_k for $k=0, 1, 2, \cdots$. The values of a_k and b_k are plotted against DW in Figures 3a and 3b, according to the sign of DW. They increase with DW. There is no real root of a_0 when $DW<0$, or b_1 when $DW<-2$. The nature of eq 5c and 5d is illustrated in Figure 4. As for the roots of eq 5c, a is real when DW is negative, and b is real when DW is less than -2. The

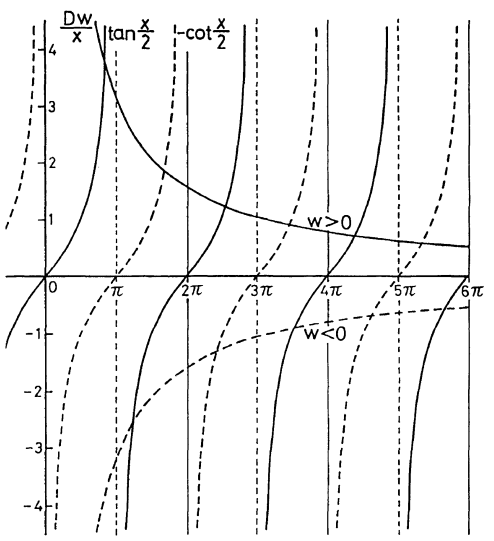

Figure 2. Graphical solutions of transcendental equations. Solid curves, $\tan(x/2)$; Dotted curves; $-\cot(x/2)$. Intersecting points correspond to solutions of eq 5a and 5b.

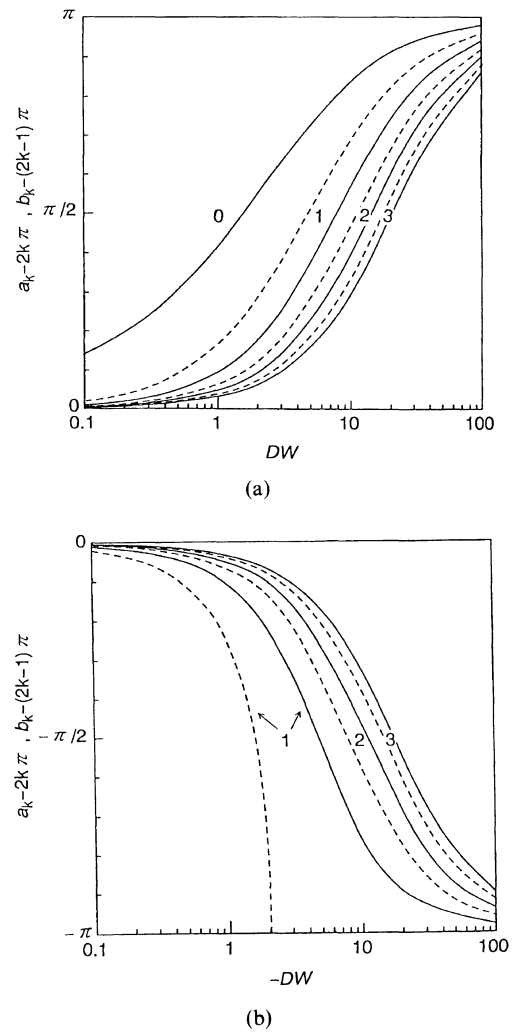

Figure 3. a_k and b_k as functions of DW. Numerical values in the figure are the values of k.

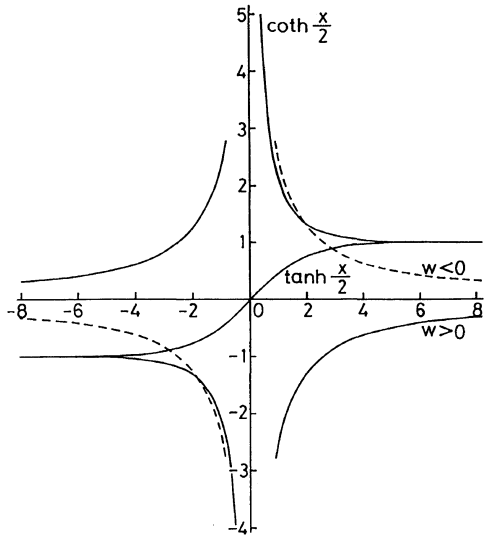

Figure 4. Graphical solutions of transcendental equation. $\tanh(x/2)$ and $\coth(x/2)$ are plotted against x. Intersecting points of these curves and the curve which represents DW/x give solutions to eq 5c and 5d.

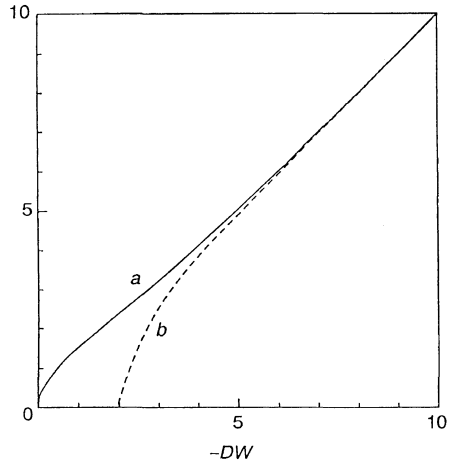

Figure 5. a and b as functions of $-DW$.

values of a and b are shown as functions of $-DW$ in Figure 5. Both values of a and b approach $-DW$ as $-DW$ increases. If we set $a_0 = ia$ and $b_1 = ib$, the last two terms in eq 4 can be replaced by the first terms of the first and second sums in eq 4, respectively. Hereafter, we use these notations for convenience.

It is of interest that the parameters, a_k, b_k depend on the value of DW, but are independent of chain dimensions. However the distribution function of the confined chain is determined not only on DW but also d_0, the square of the ratio of the radius of gyration of the unconfined chain to the interplate distance.

The Hamiltonian expression proposed by Oono was depicted as[8]

$$H=\frac{1}{2}\int_0^{N_0} dS\left(\frac{d}{dS}C(S)\right)^2 + \frac{1}{2}v_0\int_0^{N_0} dS\int_0^{N_0} dS'\,\delta(C(S)-C(S')) \times l(S,S')^{\theta-1/2} \qquad |S-S'|>c \tag{6}$$

where $C(S)$ designates the spatial position of the polymer segments at a contour length S along the chain, v_0 is the excluded volume parameter, $l(S, S')$ is the shortest contour length between $C(S)$ and $C(S')$ along the chain, assuming both ends are connected with each other, θ is the homotopy parameter, and c is the cut-off distance which is introduced to eliminate the self interaction of segments.

Using eq 6, the first order perturbation expansion of the distribution function of the perturbed chain, which starts at $\boldsymbol{R}'$ and ends at $\boldsymbol{R}$, with respect to v_0 is given as

$$G_b(\boldsymbol{R},\boldsymbol{R}';N_0)=G_0(\boldsymbol{R},\boldsymbol{R}';N_0)-v_0\int dS[\min(S,N_0-S)]^{\theta-1/2} \times\int dS'\int d\boldsymbol{R}''G_0(\boldsymbol{R}'',\boldsymbol{R}';S')G_0(\boldsymbol{R}'',\boldsymbol{R}'';S)G_0(\boldsymbol{R},\boldsymbol{R}'';N_0-S-S') =G_{0x}(R_x;N_0)G_{0y}(R_y;N_0)G_{0z}(z,z';N_0)$$

$$-v_0\int \mathrm{d}S(3/2\pi S)G_{0x}(R_x;\, N_0-S)G_{0y}(R_y;\, N_0-S)$$
$$\times I(z, z';\, S, N_0)[\min(S, N_0-S)]^{\theta-1/2} \tag{7}$$

where S is the contour length of the loop in eq 6. I is given as

$$I(z, z';\, S, N_0)=\int_0^{N_0-S}\mathrm{d}S'\int_{-D/2}^{D/2}\mathrm{d}z''G_{0z}(z'', z';\, S')G_{0z}(z'', z;\, S)G_{0z}(z, z'';\, N_0-S-S')$$
$$=12d_0(1-t)$$
$$\times\left\{\sum_k\sum_l A_kA_l\cos(a_kz/D)\cos(a_lz'/D)K_0(a_k^2d_0(1-t),\, a_l^2d_0(1-t))\right.$$
$$\times\left[\sum_m A_mJ_{klm}^{cc}\exp(-a_m^2d_0t)+B_mJ_{klm}^{cs}\exp(-b_m^2d_0t)\right]$$
$$+\sum_k\sum_l B_kB_l\sin(b_kz/D)\sin(b_lz'/D)K_0(b_k^2d_0(1-t),\, b_l^2d_0(1-t))$$
$$\left.\times\left[\sum_m A_mJ_{klm}^{sc}\exp(-a_m^2d_0t)+B_mJ_{klm}^{ss}\exp(-b_m^2d_0t)\right]\right\} \tag{8}$$

where

$$K_0(a, b)=(\exp(-b)-\exp(-a))/(a-b) \tag{9}$$

and $t=S/N_0$. The explicit forms of J_{klm} are given in the Appendix.

The value of G_b depends on the value of the cut off distance, c. In the limit to approach c to 0, the value of G_0 diverges as the value of θ approaches to 0. Removal of the unphysical sensitive dependence on the cut off distance is done by renormalization group analysis, as shown in the next section.

MEAN SQUARE END-to-END DISTANCE

Bare Perturbation

The component of the mean square end-to-end distance parallel to the plates, $\langle R_x^2\rangle$ is given as

$$\langle R_x^2\rangle=\frac{N_0}{3}+\frac{1}{3}\frac{3}{2\pi}v_0\frac{\int\mathrm{d}z\int\mathrm{d}z'I_x(z, z')}{\int\mathrm{d}z\int\mathrm{d}z'\,G_{0z}(z, z';\, N_0)} \tag{10}$$

where

$$I_x(z, z')=\int\mathrm{d}SI(z, z';\, S, N_0)[\min(S, N_0-S)]^{\theta-1/2} \tag{11}$$

Introducing eq 8 into eq 11, integrations are performed, so that

$$\int\mathrm{d}z\int\mathrm{d}z'\,I_x(z, z')=D^2N_0^{\theta-1/2}12d_0$$
$$\times\left\{\sum_k A_kf^2(a_k)g_x(a_k^2d_0)+\sum_k A_k^2f^2(a_k)T_{xk}^c(d_0)\right.$$
$$\left.+2\sum_{k<l}\sum A_kA_lf(a_k)f(a_l)T_{xkl}^c(d_0)\right\} \tag{12}$$

where

$$f(x)=\sin(x/2)/(x/2) \tag{13}$$

$$g_x(x) = \int_0^{1/2} dt(1-t)t^{\theta-1/2}\exp(-x(1-t))H^0(d_0t) + \int_{1/2}^{1} dt(1-t)^{1/2}\exp(-x(1-t))H^0(d_0t) \quad (14)$$

$$H^0(x) = \sum_m [\exp(-a_m^2x) + \exp(-b_m^2x)] \quad (15)$$

$$T^c_{xk}(d) = \exp(-a_k^2d)\left\{\sum_m A_m J^{cc}_{km} g_{x1}(a_m^2d - a_k^2d) + \sum_m B_m J^{cs}_{km} g_{x1}(b_m^2d - a_k^2d)\right\} \quad (16)$$

$$g_{x1}(x) = \int_0^{1/2} dt(1-t)t^{-1/2}\exp(-xt) + \int_{1/2}^{1} dt(1-t)^{1/2}\exp(-xt) \quad (17)$$

$$T^c_{xkl}(d) = \left\{\sum_m A_m J^{cc}_{klm}[\exp(-a_l^2d)g_{x2}(a_m^2d - a_l^2d) - \exp(-a_k^2d)g_{x2}(a_m^2d - a_k^2d)] + \sum_m B_m J^{cs}_{klm}[\exp(-a_l^2d)g_{x2}(b_m^2d - b_l^2d) - \exp(-a_k^2d)g_{x2}(b_m^2d - b_k^2d)]\right\} \Big/ (a_k^2d - a_l^2d) \quad (18)$$

$$g_{x2}(x) = \int_0^{1/2} dt\, t^{-1/2}\exp(-xt) + \int_{1/2}^{1} dt(1-t)^{-1/2}\exp(-xt) \quad (19)$$

The explicit forms of J_{km} are given in the Appendix. We put $\theta = 0$ into eq 14, 17, and 19, except for the first term in eq 14, because these terms are regular at $\theta = 0$.

$H^0(x)$ can be evaluated using the following approximation.

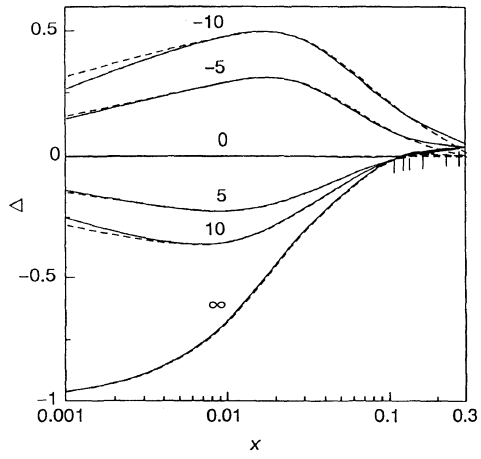

Figure 6. Verification of the approximation in eq 20. Solid curves: $\Delta = \sum_k [\exp(-a_k^2x) + \exp(-b_k^2x)] - (\pi x)^{1/2} + 1/2 + \exp(-\pi^2x) - \exp(-a_0^2x) - \exp(-b_0^2x)$. Dotted curves, $ax^b\exp(-cx)$. The numerical values in the figure are the values of DW. Vertical bars represent the values of x_0. The order left to right corresponds to decreasing values of DW.

$$H^0(x) = \begin{cases} (\pi x)^{-1/2}/2 + h_0(x) + h_1(x) & x < x_0 \\ h_1(x) & x > x_0 \end{cases} \quad (20)$$

where

$$h_0(x) = -\tfrac{1}{2} - \exp(-\pi^2x) + ax^b\exp(-cx) \quad (21a)$$

$$h_1(x) = \exp(-a_0^2x) + \exp(-b_1^2x) \quad (21b)$$

and where a, b, c, and x_0 are suitable chosen parameters.

In Figure 6, $\Delta = H^0(x) - (\pi x)^{-1/2}/2 + 1/2 + \exp(-\pi^2x) - h_1(x)$ is plotted against x for various values of DW. The dotted curves indicate the corresponding values of $ax^b\exp(-cx)$. Agreement of the solid and dotted curves is good for wide ranges of x. Equation 20 is suitable for an evaluation of the value of $H^0(x)$.

Substituting eq 20 into eq 14, and expanding the integrand with respect to θ around 0, the integral up to the 0-th order of θ can be evaluated as

$$g_x(x) = (\pi d_0)^{-1/2}/2\exp(-x)[1/\theta + g_{x00}(x)] + g_{x01}(x) \quad (22)$$

where

$$g_{x00}(x)=\int_0^{xp_0} dt[(\exp(t)-1)/t]+\ln(p_0)+[1-\exp(xp_0)]/x+\int_{1/2}^{p_1} dt(1-t)^{1/2}t^{-1/2}\exp(xt) \quad (23)$$

$$g_{x01}(x)=\int_0^{p_0} dt(1-t)t^{-1/2}h_0(d_0t)\exp(-x(1-t))+\int_{1/2}^{p_1} dt(1-t)^{1/2}h_0(d_0t)\exp(-x(1-t))+\int_0^{1/2} dt(1-t)t^{-1/2}h_1(d_0t)\exp(-x(1-t))+\int_{1/2}^{1} dt(1-t)^{1/2}h_1(d_0t)\exp(-x(1-t)) \quad (24)$$

p_O and p_1 are the parameters used to select the approximation for eq 20, and are given as

$$p_0=\min(x_0/d_0, 1/2) \quad (25a)$$

$$p_1=\max(1/2, \min(x_0/d_0, 1)) \quad (25b)$$

Renormalization

Equation 22 shows that g_x is singular at $\theta=0$. This singularity must be adsorbed in the renormalization constants. We introduce a phenomenological number of bonds, N, and a renormalized excluded volume parameter, u. The renormalization constants are defined and expanded as

$$N=Z_N N_0 \quad Z_N=1+Bu \quad (26a)$$

$$u=Z_u u_0 \quad Z_u=1+o(u) \quad (26b)$$

where $u_0=(3/2\pi)^{3/2}v_0L^{\theta}$ is the dimensionless excluded volume parameter, and L is a phenomenological coarse-grain length. Substituting eq 26a and 26b into eq 10, and expanding up to the first order of u, the singularity in the limit of $\theta\to 0$ is adsorbed by setting $B=1/\theta$.

This results in

$$\langle R_x^2\rangle=\frac{N(N/L)^u}{3}\{1+u[F_{x1}(d^*)+2(\pi d^*)^{1/2}F_{x2}(d^*)]\} \quad (27)$$

where

$$F_{x1}(d)=\left\{\sum_k A_k f^2(a_k)\exp(-a_k^2 d)g_{x00}(a_k^2 d)\right\}\Big/\left\{\sum_k A_k f^2(a_k)\exp(-a_k^2 d)\right\} \quad (28a)$$

$$F_{x2}(d)=\left\{\sum_k A_k f^2(a_k)g_{x01}(a_k^2 d)+\sum_k A_k^2 f^2(a_k)T^c_{xk}(d)+2\sum_{k<l}\sum A_k A_l f(a_k)f(a_l)T^c_{xkl}(d)\right\}\Big/\left\{\sum_k A_k f^2(a_k)\exp(-a_k^2 d)\right\} \quad (28b)$$

and

$$d^*=N(N/L)^u/6D^2 \quad (29)$$

The stable fixed point u^* is the same as that obtained in the previous paper,[7] which is given as

$$u^*=\theta/4 \quad (30)$$

For a suitable long chain in a good solvent, we use u^* instead of u.

At the limit of $D\to\infty(d\to 0)$, (as shown in the Discussions section), we get

$$g_{x00}(0)=g_\infty=-\ln 2-1+\pi/4 \quad (31)$$

and for the parallel component of the mean square end-to-end distance in an unconfined state, we get

$$\langle R_x^2\rangle_\infty=\frac{N(N/L)^u}{3}(1+(\theta/4)g_\infty) \quad (32)$$

The contribution of $(\pi d)^{1/2}F(d^*)$ is negligible. Finally, the following relation is obtained

$$\langle R_x^2\rangle/\langle R_x^2\rangle_\infty = 1+(\theta/4)[F_{x1}(d)-g_\infty+2(\pi d)^{1/2}F_{x2}(d)] \quad (33)$$

where

$$d=\langle R_z^2\rangle_\infty/2D^2 \quad (34)$$

$\langle R_z^2\rangle$ is the perpendicular component of the mean square end-to-end distance, and the suffix ∞ indicates the value in an unconfined state.

Mean Square End-to-End Distance of a Chain Where One End is Fixed

If one end of a chain is fixed at z, the parallel component of the mean square end-to-end distance of the chain, $\langle R_x^2(z)\rangle$ is given as

$$\langle R_x^2(z)\rangle = \frac{N_0}{3}+\frac{1}{3}\frac{3}{2\pi}v_0\frac{\int dz' I_x(z,z')}{\int dz' G_{0z}(z,z';N_0)} \quad (35)$$

In the same manner for $\langle R_x^2\rangle$, we get

$$\langle R_x^2(z)\rangle/\langle R_x^2\rangle_\infty = 1+(\theta/4)[F_{x1}(z/D,d)-g_\infty+2(\pi d)^{1/2}F_{x2}(z/D,d)] \quad (36)$$

where

$$F_{x1}(x,d)=\left\{\sum_k A_k\cos(a_k x)f(a_k)\exp(-a_k^2 d)g_{x00}(a_k^2 d)\right\} \Big/ \left\{\sum_k A_k\cos(a_k x)f(a_k)\exp(-a_k^2 d)\right\} \quad (37a)$$

$$F_{x2}(x,d)=\left\{\sum_k A_k\cos(a_k x)f(a_k)g_{x01}(a_k^2 d)+\sum_k A_k^2\cos(a_k x)f(a_k)T^c_{xk}(d)+\sum_{k<l}\sum A_k A_l[\cos(a_k x)f(a_l)+\cos(a_l x)f(a_k)]T^c_{xkl}(d)\right\} \Big/ \left\{\sum_k A_k\cos(a_k x)f(a_k)\exp(-a_k^2 d)\right\} \quad (37b)$$

DISCUSSIONS

Some Limiting Cases

The value of d increases as proportional to D^{-2}, with decreasing D. When D is much smaller than the mean end-to-end distance in an unconfined state, only the contribution of the terms of $k=0$ is relevant in eq 28a and 28b. Using eq 25a and 25b, we get $p_0=x_0/d$, $p_1=1/2$, and $a_0^2 dp_0=a_0^2 x_0$. All relevant terms in eq 28a are independent of d. Thus the terms in $F_{x1}(d)$ are independent of d except for $-\ln(p_0)$, which increases very gradually in proportion to $\log(d)$, with increasing d. In the same manner, we show that the value of $F_{x2}(d)$ approaches the constant $+o(D)$, with decreasing D. Then eq 33 predicts that $\langle R_x^2\rangle$ increases in proportion to D^{-1} with decreasing D for any value of W, when the polymer is confined between two plates separated by a short distance. This prediction is consistent with the results obtained by Wang *et al.*,[6] and our previous calculations.[7] However, this exponent differs from the prediction arrived at by scaling arguments[4,5] or by the mean field approximation.[8] One reason for this difference is that perturbation expansion cannot be applied when $D \ll \langle R_z^2\rangle_\infty^{1/2}$ because the values of the perturbation terms become very large.

When the limit to approach D to infinity while W is finite, the value of d approaches 0. The value of $F_{x2}(d)$ becomes constant. Then the third term in [ ]of eq 33 is negligible. The value of $g_{x00}(a_k^2 d)$ becomes equal to g_∞ for all values of k. The value of $\langle R_x^2\rangle$ approaches $\langle R_x^2\rangle_\infty$ as D increases. However, when W is negative, a approaches $-DW$ as shown in Figure 5. $a^2 d$ approaches $W^2\langle R_z^2\rangle/2$, which is both positive and finite. The contribution of this term to $F_{x1}(d)$ can be disregard in the calculation of $\langle R_x^2\rangle$, because the value of the coefficient, $A_0 f^2(a_0)\exp(-a_0^2 d)$ falls off to 0

in proportion to a^{-1} with increasing a. From eq 37a, $F_{x1}(z, d)$ can be rewritten as

$$F_{x1}(z,d)= \left\{A_0 f_0 \cosh(az/D)\exp(a^2 d) g_{x00}(a^2 d) + \sum_k f(a_k)\cos(a_k z/D)\exp(a_k^2 d) g_{x00}(0)\right\} \Big/ \left\{A_0 f_0 \cosh(az/D)\exp(a^2 d) + \sum_k f(a_k)\cos(a_k z/D)\exp(a_k^2 d)\right\} \quad (38)$$

where

$$a=-DW \quad (39a)$$

$$A_0=\frac{1}{\sinh(a)/a+1}=2a\exp(-a) \quad (39b)$$

$$f_0=\sinh(a/2)/(a/2)=\exp(a/2)/a \quad (39c)$$

and

$$a_k=(2k-1)\pi \qquad k>0 \quad (39d)$$

for suitably large values of a. Using the relation

$$\sum_k (-1)^k \frac{\cos(2k-1)x}{2k-1}=\begin{cases}\pi/4 & x<\pi/2\\ 0 & x=\pi/2\end{cases} \quad (40)$$

we get

$$F_{x1}(z,d)= \{\exp(w^2/2-wr)g_{x00}(-w^2/2)+g_\infty/4\} /\{\exp(w^2/2-wr)+1/4\} \quad (41)$$

where

$$w=-W\langle R_z^2\rangle_\infty^{1/2} \quad (42a)$$

and

$$r=(D/2-z)/\langle R_z^2\rangle_\infty^{1/2} \quad (42b)$$

Equation 41 shows that F_{x1} can be approximated as $g_{x00}(-w^2/2)$ when $r<w/2$, and as g_∞ when $r>w/2$, respectively. The crossover region between the two states is narrow. Then the effective range of the polymer plate interaction is predicted to be $w/2$ times as large as $\langle R_z^2\rangle_\infty^{1/2}$ when the interplate distance is large. Equation 41 also predicts that $\langle R_x^2(D/2)\rangle$ is continuous at $W=0$, and no phase transition can be found from the viewpoint of chain dimensions.

Crossover Behavior

The values of $\langle R_x^2\rangle/\langle R_x^2\rangle_\infty$ are plotted against $D/\langle R_z^2\rangle_\infty^{1/2}$ for various values of DW in Figure 7. Hereafter, the value of θ is placed at 1/2. In the range of $D/\langle R_z^2\rangle_\infty^{1/2}<1$, the effect of confinement is important. The value of $\langle R_x^2\rangle/\langle R_x^2\rangle_\infty$ increases rapidly as $D/\langle R_z^2\rangle_\infty^{1/2}$ decreases for any value of DW. The segments of the confined chain are squeezed in a direction parallel to the plates, by compression of the chain in this region. The value of $\langle R_x^2\rangle$ decreases monotonously, and approaches the value for an unconfined state, as $D/\langle R_z^2\rangle_\infty^{1/2}$ increases. In the range of $D/\langle R_z^2\rangle_\infty^{1/2}>1$, the effect of the repulsive polymer plate interaction becomes irrelevant. However the contribution of the attractive interaction remains relevant. $\langle R_x^2\rangle/\langle R_x^2\rangle_\infty$ is plotted against DW in Figure 8 and increases with DW, when $D/\langle R_z^2\rangle_\infty^{1/2}$ is small and W, positive. This is explained as follows. The segments are pushed into the central part between the plates by the repulsive

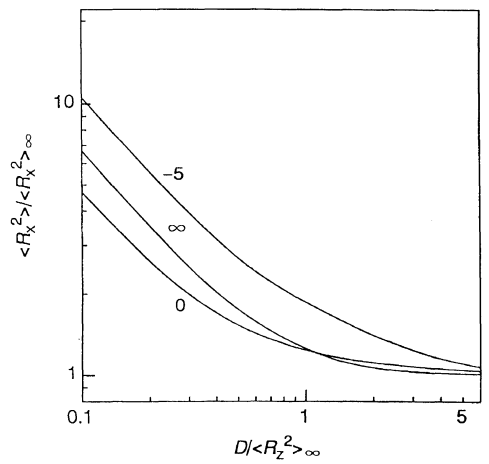

Figure 7. $\langle R_x^2\rangle/\langle R_x^2\rangle_\infty$ as functions of $D/\langle R_z^2\rangle_\infty^{1/2}$. The numerical values in the figure are the values of DW.

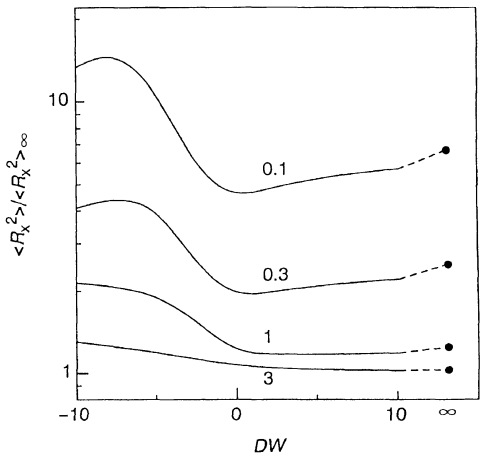

Figure 8. $\langle R_x^2\rangle/\langle R_x^2\rangle$ *vs. DW*. The numerical values in the figure are the values of $D/\langle R_z^2\rangle_\infty^{1/2}$.

polymer plates interaction. While the interplate distance is large, $\langle R_x^2\rangle/\langle R_x^2\rangle_\infty$ is insensitive to DW. When DW is negative, $\langle R_x^2\rangle/\langle R_x^2\rangle_\infty$ increases with decreasing DW. The interaction between the polymer and plates becomes more attractive, then the segments of the polymer are more adsorbed on the plate. The chain spreads along both plates when the chain dimension is much larger than D.

In Figures 9a and 9b, the values of $\langle R_x^2(z)\rangle/\langle R_x^2\rangle_\infty$ are plotted against z/D. The values of $\langle R_x^2(z)\rangle/\langle R_x^2\rangle_\infty$ are almost independent of z for small values of $D/\langle R_z^2\rangle_\infty^{1/2}$. However, they vary with z for large values of $D/\langle R_z^2\rangle_\infty^{1/2}$. It is interesting that the values of $\langle R_x^2(z)\rangle/\langle R_x^2\rangle_\infty$ of the chain where one end is anchored near the adsorbing plates are smaller than those of the chains where one end is located near the center between the plates. An intuitive interpretation is as follows. The chain segments are adsorbed by both plates when D is small and W is negative. When D becomes larger than the chain dimensions, the bridge type conformation is elongated in a direction perpendicular to the plates, and the value of $\langle R_x^2(z)\rangle$ becomes smaller than those of other conformations. However, when D is much larger than the chain dimensions, the chain is adsorbed by either of the two plates, and

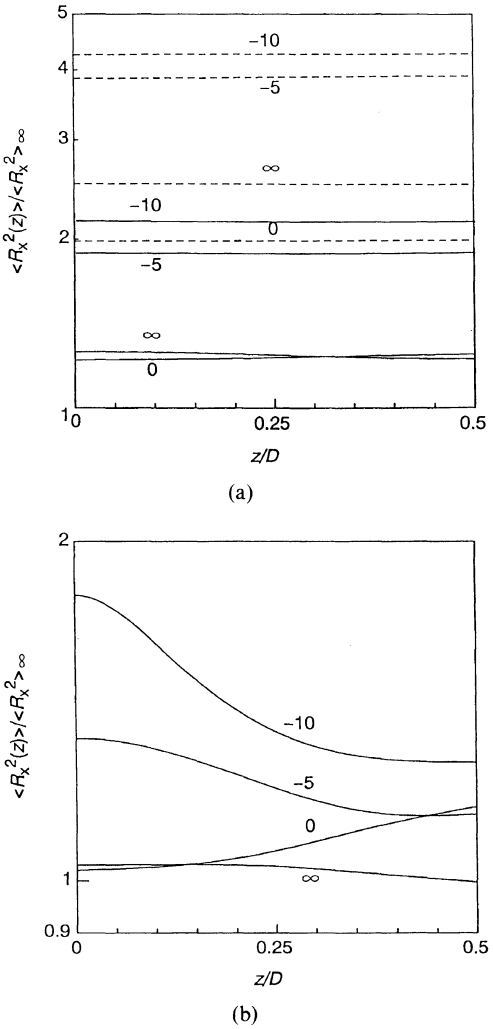

Figure 9. $\langle R_x^2(z)\rangle/\langle R_x^2\rangle_\infty$ as functions of z. Dotted curves, $D/\langle R_z^2\rangle_\infty^{1/2}=0.3$; solid curves in (a), $D/\langle R_z^2\rangle_\infty^{1/2}=1$; in (b); $D/\langle R_z^2\rangle_\infty^{1/2}=3$. The numerical values in the figure represent the values of DW.

$\langle R_x^2(D/2)\rangle$ becomes larger than $\langle R_x^2(0)\rangle$.

Acknowledgment This work was supported in part by a Grant-in-Aid from the Ministry of Education, Science, and Culture of Japan.

APPENDIX

The explicit forms of J in eq 16 and 18 are as follows.

$$J_{km}^{cc} = -f(2a_k)f(2a_m) + [f(2a_k - 2a_m) + f(2a_k + 2a_m)]/2$$

$$J_{km}^{cs} = f(2a_k)f(2b_m) - [f(2a_k - 2b_m) + f(2a_k + 2b_m)]/2$$

$$J_{km}^{sc} = f(2b_k)f(2a_m) - [f(2b_k - 2a_m) + f(2b_k + 2a_m)]/2$$

$$J_{km}^{ss} = -f(2b_k)f(2b_m) + [f(2b_k - 2b_m) + f(2b_k + 2b_m)]/2$$

$$J_{klm}^{cc} = [f(a_k - a_l - 2a_m) + f(a_k - a_l + 2a_m) + f(a_k + a_l - 2a_m) + f(a_k + a_l + 2a_m)]/2$$

$$J_{klm}^{cs} = -[f(a_k - a_l - 2b_m) + f(a_k - a_l + 2b_m) + f(a_k + a_l - 2b_m) + f(a_k + a_l + 2b_m)]/2$$

$$J_{klm}^{sc} = [f(b_k - b_l - 2a_m) + f(b_k - b_l + 2a_m) - f(b_k + b_1 - 2a_m) - f(b_k + b_l + 2a_m)]/2$$

$$J_{klm}^{ss} = -[f(b_k - b_l - 2b_m) + f(b_k - b_l + 2b_m) - f(b_k + b_1 - 2b_m) - f(b_k + b_1 + 2b_m)]/2$$

REFERENCES

1. For examples, A. Takahashi and M. Kawaguchi, *Adv. Polym. Sci.*, **46**, 1 (1982).
2. E. A. DiMarzio and R. J. Rubin, *J. Chem. Phys.*, **55**, 4318 (1971).
3. D. Chan, B. Davies, and P. Richmond, *J. Chem. Soc., Faraday Trans. 2*, **72**, 1584 (1975).
4. M. Daoud and P. G. de Gennes, *J. Physiques*, **38**, 85 (1977).
5. L. Turban, *J. Physiques*, **45**, 341 (1984).
6. Z. Wang, A. M. Nemirovsky, and K. F. Freed, *J. Chem. Phys.*, **86**, 4266 (1987).
7. K. Shiokawa, *Polym. J.*, **22**, 925 (1990).
8. K. Shiokawa, *Polym. J.*, **23**, 885 (1991).
9. Y. Oono, *Phys. Rev. A*, **30**, 986 (1984).
10. P. G. de Gennes, *Rep. Prog. Phys.*, **32**, 187 (1969).